Local proliferation dominates lesional macrophage accumulation in atherosclerosis

Published in final edited form as:
Nat Med. 2013 September ; 19(9): 1166–1172. doi:10.1038/nm.3258.

Local proliferation dominates lesional macrophage accumulation in atherosclerosis

Clinton S. Robbins[1,2,3,*], **Ingo Hilgendorf**[1,*], **Georg F. Weber**[1], **Igor Theurl**[1], **Yoshiko Iwamoto**[1], **Jose-Luiz Figueiredo**[1,4], **Rostic Gorbatov**[1], **Galina K. Sukhova**[4], **Louisa M.S. Gerhardt**[1], **David Smyth**[2], **Caleb C. J. Zavitz**[2], **Eric A. Shikatani**[2], **Michael Parsons**[5], **Nico van Rooijen**[6], **Herbert Y. Lin**[1], **Mansoor Husain**[2], **Peter Libby**[4], **Matthias Nahrendorf**[1], **Ralph Weissleder**[1,7], and **Filip K. Swirski**[1]

[1]Center for Systems Biology, Massachusetts General Hospital and Harvard Medical School, Boston, Massachusetts, USA [2]Toronto General Research Institute, University Health Network, Toronto, ON, Canada [3]Departments of Laboratory Medicine and Pathobiology and Immunology, University of Toronto, Toronto, ON, Canada [4]Cardiovascular Division, Department of Medicine, Brigham and Women's Hospital, Boston, Massachusetts, USA [5]Samuel Lunenfeld Research Institute, Mount Sinai Hospital, Toronto, ON, Canada [6]Department of Molecular Cell Biology, Free University Medical Center, Amsterdam, The Netherlands [7]Department of Systems Biology, Harvard Medical School, Boston, Massachusetts, USA

Abstract

During the inflammatory response that drives atherogenesis, macrophages accumulate progressively in the expanding arterial wall[1,2]. The observation that circulating monocytes give rise to lesional macrophages[3–9] has reinforced the concept that monocyte infiltration dictates macrophage build-up. Recent work indicates, however, that macrophages do not depend on monocytes in some inflammatory contexts[10]. We therefore revisited the mechanism of macrophage accumulation in atherosclerosis. We show that murine atherosclerotic lesions experience a surprisingly rapid, 4-week, cell turnover. Replenishment of macrophages in these experimental atheromata depends predominantly on local macrophage proliferation rather than monocyte influx. The microenvironment orchestrates macrophage proliferation via the involvement of scavenger receptor (SR)-A. Our study reveals macrophage proliferation as a key

Correspondence: F.K.S. (fswirski@mgh.harvard.edu), Center for Systems Biology, Massachusetts General Hospital, Harvard Medical School, Simches Research Building, 185 Cambridge St., Boston, MA 02114; phone, 617-724-6242, fax, 617-726-5708. C.S.R. (clint.robbins@utoronto.ca), Division of Advanced Diagnostics, Toronto General Research Institute, University Health Network, Toronto Medical Discovery Tower, 101 College St., Toronto, ON M5G1L7; phone, 416-581-7510.
*authors contributed equally

Authors contributions

C.S.R. and I.H. conceived the project, designed and performed experiments, analyzed and interpreted data. G.F.W., I.T., L.M.S.G, D.S., C.J.Z., E.A.S performed experiments and helped to interpret the data; J.L.F., R.G., I.H. performed animal surgeries; Y.I. performed the immunofluorescence histology and immunohistochemistry; M.P. performed ImageStreamX™ Mark II studies; G.K.S., P.L., M.N., M.H. and R.W. provided materials, intellectual input, and edited the manuscript; N.v.R. provided clodronate liposomes; H.Y.L. edited the manuscript. F.K.S. conceived the project, designed experiments, and supervised the study. C.S.R. and F.K.S. wrote the manuscript.

Author information

The authors declare no competing financial interests. Correspondence and requests for materials should be addressed to F.K.S. (fswirski@mgh.harvard.edu), Center for Systems Biology, Massachusetts General Hospital, Harvard Medical School, Simches Research Building, 185 Cambridge St., Boston, MA 02114; phone, 617-724-6242, fax, 617-643-6133 or C.S.R. (clint.robbins@utoronto.ca), Division of Advanced Diagnostics, Toronto General Research Institute, University Health Network, Toronto Medical Discovery Tower, 101 College St., Toronto, ON M5G1L7; phone, 416-581-7510.

event in atherosclerosis and identifies macrophage self-renewal as a therapeutic target for cardiovascular disease.

Over the last 30 years macrophages have emerged as protagonists of atherosclerosis and its complications. Macrophages amass in lesions, ingest lipids, and produce a diverse repertoire of inflammatory mediators that exacerbate disease[1,2]. In the mouse, lesional macrophages arise predominantly from circulating Ly-6C^{high} monocytes[5–7,11–13]. These insights have contributed to the perception that macrophages gradually accrue in atherosclerotic lesions whereby a single infiltrating monocyte yields one terminally-differentiated macrophage. Recent observations that monocyte kinetics in acute injury are rapid[14], that tissue macrophages may not depend on monocytes[10,15], and that the adventitia harbors hematopoietic progenitors[16] reveal potential alternative explanations for how atherosclerosis evolves. The prevailing models, therefore, require reevaluation.

Do lesional macrophages in atherosclerosis accumulate gradually or turn over rapidly? To answer, we subcutaneously implanted osmotic pumps containing the thymidine analogue 5-bromo-2′-deoxyuridine (BrdU) in 4-month old apolipoprotein E-deficient (*Apoe*$^{-/-}$) mice consuming a high cholesterol diet (HCD) for 8 weeks. BrdU incorporates into newly synthesized DNA and thus reports on a cell's, or its progenitor's, proliferative history. Nearly all (92±1%) aortic macrophages, identified as Lin$^-$ CD11b$^+$CD11c$^{low\text{-}neg}$F480^{high} cells by flow cytometry (Fig. 1a), stained for BrdU after 4 weeks (when mice were 5 months old) (Fig. 1b and c). Immunofluorescence experiments identified Mac3$^+$BrdU$^+$ macrophages within the plaque intima and adventitia (Fig. 1d–f). This low-level BrdU administration had no intrinsic effect on macrophage turnover kinetics because the rate of BrdU signal decay following pump removal closely approximated its rate of incorporation (Fig. 1c). Despite observed increases in lesion size (Fig. 1g), aortic root macrophage burden did not change significantly during BrdU labeling (Fig. 1h), suggesting that, at this stage of atherosclerosis, cell loss processes counterbalance macrophage renewal. These data identify a previously unrecognized dynamic in the mononuclear phagocytic response during atherosclerosis and reveal remarkably rapid macrophage turnover in lesions.

Lesional macrophages could replenish either through the continuous recruitment of circulating monocytes or through some other processes. We assessed lesional macrophage accumulation in *Apoe*$^{-/-}$ HCD mice depleted of circulating monocytes for 5 d (Fig. 2a) and found, unexpectedly, that monocyte depletion had no effect, not only on incorporation of BrdU by lesional macrophages (Fig. 2b and c) but also on the number of total macrophages (Fig. 2d) and total lesion area (Supplementary Fig. 1a). To examine the relationship between blood monocytes and tissue macrophages in more detail, 4-month old CD45.1$^+$ *Apoe*$^{-/-}$ HCD and CD45.2$^+$ *Apoe*$^{-/-}$HCD mice (8 weeks of Western diet) were joined for 5 weeks by parabiosis, a procedure that allows circulating cells to enter partner tissues[17]. The procedure did not alter the frequency of monocytes in the blood (Supplementary Fig. 1b) and had no effect on BrdU incorporation in lesional macrophages (Supplementary Fig. 1c). Whereas Ly-6C^{high} monocyte chimerism in the blood (30±5%), spleen (26±4%), and aorta (25±6%) was high – and typical of monocyte chimerism at equilibrium[18] – macrophage chimerism in the aorta was low (5±2%) (Fig. 2e–g). Therefore, in established disease, the discrepancy between monocyte and macrophage chimerism illustrates either slow macrophage replenishment or macrophage replenishment that does not rely exclusively on monocyte influx. Because macrophages replenish rapidly in established disease (~4 weeks, Fig. 1), macrophage accumulation likely occurs through processes other than monocyte infiltration. Surgical separation of parabionts provided complementary evidence in support of this conclusion. Separation led to a decline in monocyte chimerism in blood, spleen and aorta, but chimerism among lesional macrophages remained unchanged for at least 2 weeks (Fig.

2h). Together, these data show that monocyte recruitment cannot fully account for lesional macrophage accumulation in established atherosclerosis.

Macrophage turnover that is largely independent of monocytes does not preclude the initial development of plaque macrophages from hematopoietic precursors. To determine when monocytes and macrophages converge, relatively young (early atherosclerosis) mice were joined in parabiosis for 1 and 4 weeks. Unlike established disease (Fig. 2e–g), monocyte and macrophage chimerism in these mice was similar (Supplementary Figure 2a), which is aligned with previous observations that early development of atherosclerotic lesions depends on monocyte recruitment[19]. To determine if monocytes and macrophages converge in established disease, we lethally irradiated and reconstituted 4-month old CD45.2^{+}*Apoe*$^{-/-}$ HCD mice with bone marrow from CD45.1^{+}*Apoe*$^{-/-}$ mice. Over 5 months, lesional macrophages in these animals with established plaques were eventually replenished by donor-derived CD45.1^{+} cells (Supplementary Fig. 2b). These data suggest that, even though rapid lesional macrophage turnover does not require constant monocyte influx, aortic macrophages ultimately derive from a circulating precursor.

The recent identification of hematopoietic progenitors in the aortic adventitia[16] raised the possibility that lesional macrophages arise from circulating intima-seeded multipotent hematopoietic stem and progenitor cells (HSPC). To address this, we performed granulocyte-macrophage colony forming experiments on aortic tissue. As shown previously[11], HSPC were highly active in the bone marrow and spleen of *Apoe*$^{-/-}$ HCD mice (Fig. 3a). The entire aorta, on the other hand, yielded no more than 2 macrophage colonies per animal. These data accord with the recent study on HSPC activity in the vascular wall[16], and indicate that local hematopoiesis of a multiproliferative progenitor contributes minimally to lesional macrophage accumulation in atherosclerosis.

Macrophage proliferation in atherosclerotic lesions has been identified in humans, rabbits and mice[20–26] but its importance relative to monocyte recruitment has not been evaluated. We addressed this by several independent and complementary approaches. First, we adoptively transferred Ly-6C^{high} monocytes from GFP^{+} mice to *Apoe*$^{-/-}$ mice consuming HCD. 24 h following transfer, we also injected BrdU to track proliferation. 2 d after BrdU pulse, non-proliferating BrdU^{-}GFP^{+} monocytes were detected in the recipient blood (Fig. 3b). In the aorta, GFP^{+} cells grouped into F480^{low} BrdU^{-} cells, representing a few monocytes that had accumulated but neither differentiated nor proliferated, and F480^{high} cells, representing monocyte-derived macrophages, some of which had proliferated locally (BrdU^{+}) (Fig. 3b). The data indicate that proliferating lesional macrophages derive from non-proliferating circulating monocytes. Future studies will need to determine whether lesion-infiltrating monocytes, in addition to differentiation, die locally or exit. Second, we performed a 2 h *in vivo* BrdU-pulse labeling experiment, used previously to detect neointimal dendritic cell proliferation[19]. At a time when circulating monocytes had not yet incorporated BrdU (Supplementary Fig. 3a), macrophages in both *Apoe*$^{-/-}$ (Fig. 3c) and Low Density Lipoprotein Receptor-deficient (*Ldlr*$^{-/-}$) (Supplementary Fig. 3b) mice were already BrdU^{+}, indicating local proliferation. Third, analysis of the S and G_2/M phases of the cell cycle using the intercalating dye 4′,6-diamidino-2-phenylindole (DAPI) revealed a high percentage of proliferating aortic macrophages in *Apoe*$^{-/-}$mice consuming a high cholesterol diet (Fig. 3d). This finding contrasted with macrophages from wild type (WT) and young (2 month old) chow-fed *Apoe*$^{-/-}$ mice, which proliferated less, and monocytes, which did not proliferate under any circumstances (Fig. 3b, d, e). Fourth, positive staining of gated G_2/M-phase lesional macrophages for phospho-histone H3 confirmed mitosis (Fig. 3f). Fifth, to directly visualize cell division, we utilized the ImageStream$X^{™}$ Mark II platform, an approach that links multi-parameter flow cytometry with single cell immuno-fluorescence imaging. Analysis of *Apoe*$^{-/-}$ HCD mice showed G_2/M-phase aortic

macrophages in various phases of mitosis (Fig. 3g). Sixth, immunofluorescence of aortic root sections showed numerous intimal $Mac3^+$ macrophages staining positive for the nuclear proliferation antigen Ki67 (Fig. 3h). The key to interpreting these last four experiments is the ability of DAPI, phospho-histone H3, and Ki67 to identify currently – rather than formerly – proliferating cells. The colocalization of markers of cell division with mature macrophage markers (F480 by flow cytometry and Mac3 by immunofluorescence) indicates that lesional macrophages proliferate. Finally, immunohistochemistry of atherosclerotic plaques from human carotid arteries revealed Ki67-expressing oil red O^+ and $CD68^+$ lesional macrophages (Supplementary Fig. 3c), indicating that in situ proliferation of mature intimal macrophages occurs in experimental and human atherosclerosis. While classic studies have shown that the dominant proliferative cell type in the human intima is the monocyte/macrophage in both early[23] and advanced atherosclerosis[21,22], it remains to be determined whether local macrophage proliferation contributes substantially to human lesion growth, turnover, and rupture.

To quantify the contribution of local proliferation to macrophage accumulation in established atherosclerotic lesions, 4 month-old $CD45.1^+$ *Apoe*$^{-/-}$ HCD and $CD45.2^+$ *Apoe*$^{-/-}$ HCD (8 weeks on diet) mice were joined by parabiosis and implanted with BrdU-containing osmotic pumps for 4 weeks (Fig. 3i). This experiment allowed assessment of macrophage chimerism exclusively in newly accumulating $BrdU^+$ macrophages. Among newly accumulating macrophages in $CD45.1^+$ aortas, only 4% were $CD45.2^+$ (Fig. 3i), which agrees with our previous observations and further argues against macrophage residential longevity as the determining factor for low chimerism (Fig. 2e and f). Aortic chimerism alone underestimates the overall contribution of circulating monocytes because monocyte chimerism in the blood, even at equilibrium, is only ~30% (Fig. 3i). Therefore, assuming that individual $CD45.1^+$ and $CD45.2^+$ cells can infiltrate lesions equally, for every partner-derived (i.e., $CD45.2^+$) monocyte that entered the $CD45.1^+$ aorta, ~2 endogenous (i.e., $CD45.1^+$) monocytes also entered. Hence, the total contribution of the circulation ($CD45.1^+$ and $CD45.2^+$) to macrophage accumulation in a 4-week period in established disease can be, at most, ~13% (Fig. 3j). Local proliferation, which accounts for the remaining ~87% of newly-labeled $BrdU^+$ macrophages, dominates macrophage accumulation in established atherosclerosis (Fig. 3j). Similar studies conducted during early atherosclerosis, when lesional macrophage burden was still minimal (Supplementary Fig. 2a), demonstrated a larger contribution of recruited monocytes to macrophage accumulation (Fig. 3j). Collectively, these data show that, as atherosclerosis progresses, macrophage turnover becomes increasingly dependent on local proliferation of lesional macrophages.

Since lesional macrophages reside in a tissue context, macrophage proliferation might depend on the local microenvironment. We addressed this possibility with several approaches. First, we joined 4 month-old WT (C57BL6/J, $CD45.1^+$) and *Apoe*$^{-/-}$($CD45.2^+$) HCD mice by parabiosis. The joined heterogenic partners consumed a high cholesterol diet for 5 weeks. During this period, atherosclerotic lesions persisted in *Apoe*$^{-/-}$ partners but did not develop in WT partners. Among the cells accumulating in aortas, lesional macrophage chimerism remained low (Fig. 4a), although the WT aorta contained fewer total cells. Whatever the cell's origin (host or partner, *Apoe*$^{-/-}$ or WT) macrophages accumulating in *Apoe*$^{-/-}$ mice were more likely to proliferate compared to macrophages accumulating in WT mice (Fig. 4a and b). We also assessed macrophage proliferation in *Apoe*$^{-/-}$ HCD mice in different aortic segments of the same animal. Proliferation was highest among macrophages located in the aortic root and arch (where lesions are most abundant), intermediate among macrophages located in the thoracic aorta (intermediate abundance), and lowest in the abdominal aorta (least abundance) (Supplementary Fig. 4). To discriminate between lesional and adventitial macrophage proliferation, the intima was separated from the vessel wall, as previously described[27]. Whereas adventitial macrophages proliferated at a rate similar to

that observed in young non-atherosclerotic mice, lesional macrophages proliferated at a high rate (Fig. 4c). Thus, the microenvironment influences macrophage proliferation.

By what mechanism are lesional macrophages proliferating? Neither neutralizing antibody nor genetic studies targeting GM-CSF affected macrophage proliferation (Supplementary Fig. 5a and b), which was somewhat surprising given the growth factor's known role in macrophage differentiation and neointimal DC proliferation[19]. We turned our attention to the type 1 scavenger receptor class A (SR-A, also known as Msr1), which is expressed on lesional macrophages[28,29], recognizes modified low-density lipoproteins[30], and correlates with macrophage proliferation[31]. We generated mixed chimeric mice by irradiating and reconstituting *Ldlr*$^{-/-}$ mice with a mixture of WT CD45.1^{+} and *Msr1*$^{-/-}$ CD45.2^{+} bone marrow cells (Fig. 4d). This approach allowed us to compare proliferation of Msr1-competent and deficient macrophages in the same lesional microenvironment. After 16 wk of HCD, bone marrow transplantation was associated with engraftment and circulation of moderately fewer *Msr1*$^{-/-}$CD45.2^{+} monocytes compared to WT CD45.1^{+} monocytes (Supplementary Fig. 5c). In the aorta, we observed ~60% fewer *Msr1*$^{-/-}$CD45.2^{+} macrophages compared to WT CD45.1^{+} cells (Supplementary Fig. 5d) When animals were pulsed with BrdU for 2h, circulating monocytes were almost entirely BrdU^{-} regardless of genotype (Fig. 4e). Compared to WT cells, *Msr1*$^{-/-}$ macrophages proliferated less (Fig. 4f) and BrdU^{+} *Msr1*$^{-/-}$ macrophages were far less abundant in lesions (Fig. 4g). These data indicate that Msr1 contributes to the life cycle of proliferating macrophages in established atherosclerosis. Future work will need to elucidate whether the effect is direct or indirect, and investigate the mechanistic links between Msr1-mediated apoptosis, ER stress, and proliferation[31,32].

The finding that local macrophage proliferation contributes substantially to lesional macrophage accumulation prompted us to test whether interference with proliferation can reduce established atherosclerosis. *Apoe*$^{-/-}$ HCD mice received the cell cycle inhibitor fluorouracil (5-FU). It is known that 5-FU decreases the production of monocytes[33]. However, the drug was delivered for only 4 weeks, a period of time in which monocytes contribute little to macrophage accumulation in established atherosclerosis. 5-FU significantly decreased the rate (Supplementary Fig. 6a) and number (Supplementary Fig. 6b) of proliferating aortic macrophages. The overall effect of 5-FU resulted in fewer Mac3^{+} macrophages and smaller lesions (Supplementary Fig. 6 c–e). These data are consistent with studies in which genetic disruption of tumor suppressor genes and cell cycle regulators promoted macrophage proliferation and increased atherosclerosis[34,35]. These findings demonstrate that cellular proliferation is a dominant feature of atherosclerotic development and a potent therapeutic target.

Atherosclerosis is a lipid-driven inflammatory disease characterized by monocyte recruitment and differentiation[1]. When lesions regress, monocyte recruitment is suppressed[13]. Our study builds on this paradigm by providing evidence that, in addition to monocyte recruitment and differentiation, monocyte-derived lesional macrophages proliferate. Atherosclerosis develops, our data indicate, via a multiphasic numerical escalation of the monocyte-macrophage lineage. Its sequence can be summarized as follows: (1) hematopoietic stem cells proliferate in the bone marrow and spleen and give rise to monocytes[11,36,37]; (2) Monocytes circulate, infiltrate, and differentiate to macrophages[5–7,13]; (3) Lesional macrophages proliferate and locally augment their numbers in plaques (Fig. 4h). The evidence for substantial local expansion of mononuclear phagocytes resulting from proliferation within the intimal lesion adds a new dimension to our understanding of lesional leukokinetics. Moving forward, it will be important to evaluate the importance of local macrophage proliferation in human atherosclerosis, and to determine

how interfering with monocyte recruitment and macrophage proliferation at various stages of atherosclerosis affects plaque progression.

Online Methods

Animals

C57BL/6J (wild-type, WT), B6.SJL-PtprcaPep3b/BoyJ (CD45.1$^+$), apolipoprotein E–deficient (*Apoe*$^{-/-}$; B6.129P2-Apoe^{tm1Unc}), low density lipoprotein-deficient (*Ldlr*$^{-/-}$; B6.129S7-Ldlr^{tm1Her}/J) and macrophage scavenger receptor 1-deficient (*Msr1*$^{-/-}$; B6.Cg-Msr1^{tm1Csk}/J) mice were purchased from The Jackson Laboratories. Mice deficient in the β-subunit of the granulocyte-macrophage colony stimulating factor receptor (*Csf2rb*$^{-/-}$) were kindly provided by Dr. Jeffrey Whitsett at Cincinnati Children's Hospital Medical Center. *Apoe*$^{-/-}$CD45.1$^+$ were generated after backcrossing *Apoe*$^{-/-}$ mice to C57BL/6 CD45.1$^+$. At 6–8 wk of age, *Apoe*$^{-/-}$ mice were placed on a "Western" diet (high cholesterol diet, HCD) (21.2% fat weight^{-1}; 0.2% cholesterol) (Harlan Teklad, Madison, WI) or remained on a chow diet for durations listed in the manuscript. *Ldlr*$^{-/-}$ mice were fed a high fat/cholesterol diet (D12108C: 20% fat/weight; 1.25% cholesterol) (Research Diets Inc., New Brunswick, NJ). All mice were female except Ldlr$^{-/-}$, which were male. All protocols were approved by the Institutional Animal Care and Use Committee (IACUC), Subcommittee on Research Animal Care (SRAC), Massachusetts General Hospital, Charlestown, MA.

Animal models and *in vivo* interventions

BrdU incorporation studies: BrdU was administered using osmotic mini-pumps implanted subcutaneously (Alzet model 1002) at a dose of 50 μg day^{-1} or injected i.v. at 1mg mouse^{-1}. Monocyte depletion: Mice were i.v. injected daily with 200 μl clodronate loaded liposomes. Clodronate was a gift from Roche and was incorporated into liposomes are described previously[38]. Parabiosis: The procedure, adapted from[17] was conducted as previously described[39]. Briefly, after shaving the corresponding lateral aspects of each mouse, matching skin incisions were made from behind the ear to the tail of each mouse, and the subcutaneous fascia was bluntly dissected to create about 0.5 cm of free skin. The scapulas were sutured using a mono-nylon 5.0 (Ethicon, Albuquerque, NM), and the dorsal and ventral skins were approximated by continuous suture. Mice were joined for intervals of 4 to 5 weeks. In one set of experiments, after an interval of 5 weeks joined, parabiosed mice were surgically separated by a reversal of the procedure. Percent chimerism in the blood and aortic tissue was defined for either gated monocytes or macrophages as %CD45.1$^+$ (%CD45.1$^+$ & %CD45.2$^+$)$^{-1}$ in CD45.2$^+$ mice, and as %CD45.2$^+$ (%CD45.2$^+$ & %CD45.1$^+$)$^{-1}$ in CD45.1$^+$ mice. Bone marrow chimeras: *Ldlr*$^{-/-}$ HCD mice with established atherosclerosis were lethally irradiated (950cGy) and reconstituted with CD45.1$^+$ wild type (WT) bone marrow. For generation of mixed chimeras naive *Ldlr*$^{-/-}$ mice were lethally irradiated and reconstituted with a 50:50 mix of bone marrow cells from CD45.1$^+$ wild type mice and CD45.2$^+$ knockouts for SR-A I/II (*Msr1*$^{-/-}$) and the GM-CSF receptor β-chain (*Csf2rb*$^{-/-}$) respectively. Adoptive transfer: Ly-6C^{high} CD115$^+$ monocytes were sorted from GFP$^+$ mice. 3 × 10^6 cells were injected i.v. into *Apoe*$^{-/-}$ mice consuming HCD for 12 weeks. Treatment: Fluorouracil (5-FU) (APP Pharmaceuticals, LLC, USA) was administered via osmotic mini-pumps at a dose of 15 mg kg^{-1} per day for 4 weeks with two intermittent boluses of 100 mg kg^{-1} iv. Anti-GM-CSF antibody (functional grade MP1-22E9, eBioscience) was delivered i.v. at a dose of 100 μg (mouse day)$^{-1}$.

Cells

Peripheral blood for flow cytometric analysis was collected by cardiac puncture, using a 50 mM EDTA solution as anticoagulant. Erythrocytes were lysed using BD FACS Lysing Solution (BD Biosciences). Total white blood cell count was determined by preparing a 1:10

dilution of (undiluted) peripheral blood obtained from the orbital sinus using heparin-coated capillary tubes in RBC Lysis Buffer (BioLegend). After organ harvest, single cell suspensions were obtained as follows: for bone marrow, femur and tibia of one leg were flushed with PBS. Spleens were homogenized through a 40 μm-nylon mesh, after which erythrocyte lysis was performed on the spleens using RBC Lysis Buffer (BioLegend). For aortic tissue, the entire aorta was digested (from the root to the iliac bifurcation) according to a method previously published[40]. The procedure involves perfusion of the aorta (20 ml PBS) prior to digestion. Aortic tissue was cut in small pieces and subjected to enzymatic digestion with 450 U ml^{-1} collagenase I, 125 U ml^{-1} collagenase XI, 60 U ml^{-1} DNase I and 60 U ml^{-1} hyaluronidase (Sigma-Aldrich, St. Louis, MO) for 1 h at 37 °C while shaking. Total viable cell numbers were obtained using Trypan Blue (Cellgro, Mediatech, Inc, VA). To separate intimal lesions from the media and adventitia we adapted the method previously described by Butcher et al[27]. In brief, aortas were cut open longitudinally and pinned onto black wax with the intimal area facing upwards. A thin film of enzymatic digestion mixture was applied directly onto the exposed intima. After 15 min of incubation at room temperature lesions were scraped off the underlying media with a glass coverslip. Lesional tissue and the remaining media and adventitia were cut into small pieces and separately digested for 40 min at 37 °C while shaking as described above. Tissue colony forming cell assay: To determine the number of myeloid colony-forming units, a single cell suspension was prepared from bone marrow, spleens and aortic tissue and 1×10^5 cells were plated in triplicates in complete methylcellulose medium (MethoCult GF M3434, Stemcell Technologies). Counts were performed after 8 d of culture. At least three independent samples per group were analyzed.

Flow Cytometry

The following antibodies were used for flow cytometric analyses: anti-CD90.2-PE, 53–2.1 (BD Biosciences); anti-B220-PE, RA3-6B2 (BD Biosciences); anti-CD49b-PE, DX5 (BD Biosciences); anti-NK1.1-PE, PK136 (BD Biosciences); anti-Ly-6G-PE, 1A8 (BD Biosciences); anti-TER119-PE, TER119 (BD Biosciences); anti-CD11b-APCcy7, M1/70 (BD Biosciences); anti-CD11c-Alexa Fluor 700, HL3 (BD Biosciences); anti-IA^b-Percp Cy5.5, AF6-120.1 (BD Biosciences); anti-F480-PE-Cy7, BM8 (BioLegend); anti-CD45.2-FITC, 104 (BD Biosciences); anti-CD45.1-APC, A20 (BD Biosciences); anti-CD115-APC, AFS98 (ebioscience). Antibody dilutions were 1:300 – 1:700. Cell cycle analysis was carried out using FxCycle violet stain (Invitrogen). Contribution of newly-made cells to different cell populations was determined by *in vivo* labeling with bromodeoxyuridine (BrdU) (BD Biosciences). Incorporation was measured using either FITC or APC-conjugated anti-BrdU antibodies according to the manufacturer's instructions. Monocytes and macrophages were identified similarly as described previously[39]. Specifically, monocytes were identified as $CD11b^{hi}$ Lin^- (Lin = CD90/B220/CD49b/NK1.1/Ly-6G/Ter119) $F480^{lo}$. Macrophages were identified as $CD11b^{hi}$ Lin^{lo} $F480^{hi}$ $CD11c^{lo\text{-}neg}$. Data were acquired on an LSRII (BD Biosciences) and analyzed with FlowJo v8.8.6 (Tree Star, Inc.). The ImageStream$X^{™}$ imaging flow cytometry platform was used to analyze the cell cycle as per manufacturer's instructions.

Histology

Atherosclerotic plaque specimens were obtained from patients undergoing carotid endarterectomies. Carotid tissue was obtained from cardiac transplants by protocols approved by the Human Investigation Review Committee at the Brigham and Women's Hospital. Specimens were immediately immersed in saline solution, transported to the laboratory on ice (within 1 hr), embedded in OCT compound, and stored at −80°C freezer until use. Serial cryostat sections (5 μm) are cut, air dried onto microscope slides (Fisher Scientific, Pittsburgh, PA) and used for immunohistochemistry. Mouse aortae were excised,

embedded in O.C.T. compound (Sakura Finetek), and flash-frozen in isopentane and dry ice. Aortic roots were sectioned into 5 um slices, generating ~30–40 sections that spanned the entirety of the aortic root. For comparison of lesion size between the groups, sections that captured the maximum lesion area were used. Immunofluorescence double staining was carried out using BrdU Flow Kits (BD Biosciences), Mac-3: clone M3/84 (BD Biosciences) and FITC-Ki67: clone SP6 (Abcam). For BrdU immunofluorescence double staining, the sections were stained with Mac-3 antibody followed by a biotinylated secondary antibody and streptavidin-Texas Red (GE Healthcare). To denature DNA, the sections were incubated with 2 N HCl for 10 min at room temperature and for 20 min at 37 °C. Acid neutralization was achieved by immersing sections in 0.1M borate buffer. Cover slips were placed over specimens using mounting medium containing DAPI (Vector Laboratories) to identify cell nuclei. Images capture was performed using an epifluorescence microscope (Nikon Eclipse 80i, Nikon Instruments Inc.) equipped with a Cascade Model 512B camera (Roper Scientific). For immunohistochemistry, anti-CD45.1: clone A20 (eBioscience), anti-CD45.2: clone 104 (BioLegend), anti-Mac-3: clone M3/84 (BD Biosciences) was used for mouse aortic root sections, and anti-Ki67 (abcam), anti-CD68: clone KP1 (Dako) were used to stain human carotid arteries. In order to block endogenous peroxidase activity, tissue sections were pre-treated with 0.3% hydrogen peroxide solution. Following application of the appropriate biotinylated secondary antibodies, samples were developed using the Vectastain ABC kit (Vector Laboratories) and either AEC (DakoCytomation) or DAB (Vector Laboratories) substrates. Sections were counterstained with Harris Hematoxylin and specificity of staining was confirmed using relevant isotype controls. Masson trichrome (Sigma) and Oil Red O (Sigma) staining were performed to visualize collagen and lipid content, respectively. Hematoxylin and eosin (H&E) staining was performed to assess overall tissue morphology. Images were digitized using a Nanozoomer 2.0RS (Hamamatsu).

Statistics

Results were expressed as mean ± SEM. Statistical tests included unpaired Student's t test using Welch's correction for unequal variances and 1-way ANOVA followed by Tukey's or Newman-Keuls Multiple Comparison Test. P values of 0.05 or less were considered to denote significance.

Supplementary Material

Refer to Web version on PubMed Central for supplementary material.

Acknowledgments

The authors thank M. Greene for secretarial assistance. This work was supported in part by US National Institutes of Health grants 1R01HL095612 (to F.K.S.) and HHSN 268201000044C, P01-A154904, U24-CA092782, P50-CA086355 (to R.W.), and start-up funding provided by the Heart and Stroke Richard Lewar Centre of Excellence in Cardiovascular Research and the Department of Laboratory Medicine and Pathobiology, University of Toronto (to C.S.R.). C.S.R. was supported by the MGH Executive Committee on Research (ECOR) Postdoctoral Award. G.F.W. and I.H. were supported by the German Research Foundation. I. T. was supported by the Max Kade Foundation. L.M.S.G. was supported by the Boehringer Ingelheim Funds.

References

1. Swirski FK, Nahrendorf M. Leukocyte behavior in atherosclerosis, myocardial infarction, and heart failure. Science. 2013; 339:161–166. [PubMed: 23307733]
2. Hansson GK, Libby P. The immune response in atherosclerosis: a double-edged sword. Nat Rev Immunol. 2006; 6:508–519. [PubMed: 16778830]

3. Kim CJ, et al. Polymerase chain reaction-based method for quantifying recruitment of monocytes to mouse atherosclerotic lesions in vivo: enhancement by tumor necrosis factor-alpha and interleukin-1 beta. Arterioscler Thromb Vasc Biol. 2000; 20:1976–1982. [PubMed: 10938020]
4. Lessner SM, Prado HL, Waller EK, Galis ZS. Atherosclerotic lesions grow through recruitment and proliferation of circulating monocytes in a murine model. Am J Pathol. 2002; 160:2145–2155. [PubMed: 12057918]
5. Swirski FK, et al. Monocyte accumulation in mouse atherogenesis is progressive and proportional to extent of disease. Proc Natl Acad Sci U S A. 2006; 103:10340–10345. [PubMed: 16801531]
6. Swirski FK, et al. Ly-6Chi monocytes dominate hypercholesterolemia-associated monocytosis and give rise to macrophages in atheromata. J Clin Invest. 2007; 117:195–205. [PubMed: 17200719]
7. Tacke F, et al. Monocyte subsets differentially employ CCR2, CCR5, and CX3CR1 to accumulate within atherosclerotic plaques. J Clin Invest. 2007; 117:185–194. [PubMed: 17200718]
8. Combadiere C, et al. Combined inhibition of CCL2, CX3CR1, and CCR5 abrogates Ly6C(hi) and Ly6C(lo) monocytosis and almost abolishes atherosclerosis in hypercholesterolemic mice. Circulation. 2008; 117:1649–1657. [PubMed: 18347211]
9. Saederup N, Chan L, Lira SA, Charo IF. Fractalkine deficiency markedly reduces macrophage accumulation and atherosclerotic lesion formation in CCR2-/- mice: evidence for independent chemokine functions in atherogenesis. Circulation. 2008; 117:1642–1648. [PubMed: 18165355]
10. Jenkins SJ, et al. Local macrophage proliferation, rather than recruitment from the blood, is a signature of TH2 inflammation. Science. 2011; 332:1284–1288. [PubMed: 21566158]
11. Robbins CS, et al. Extramedullary hematopoiesis generates Ly-6C(high) monocytes that infiltrate atherosclerotic lesions. Circulation. 2012; 125:364–374. [PubMed: 22144566]
12. Swirski FK, Weissleder R, Pittet MJ. Heterogeneous In Vivo Behavior of Monocyte Subsets in Atherosclerosis. Arterioscler Thromb Vasc Biol. 2009
13. Potteaux S, et al. Suppressed monocyte recruitment drives macrophage removal from atherosclerotic plaques of Apoe-/- mice during disease regression. J Clin Invest. 2011; 121:2025–2036. [PubMed: 21505265]
14. Leuschner F, et al. Rapid monocyte kinetics in acute myocardial infarction are sustained by extramedullary monocytopoiesis. J Exp Med. 2012; 209:123–137. [PubMed: 22213805]
15. Schulz C, et al. A lineage of myeloid cells independent of Myb and hematopoietic stem cells. Science. 2012; 336:86–90. [PubMed: 22442384]
16. Psaltis PJ, et al. Identification of a monocyte-predisposed hierarchy of hematopoietic progenitor cells in the adventitia of postnatal murine aorta. Circulation. 2012; 125:592–603. [PubMed: 22203692]
17. Bunster EMRK. An Improved Method of Parabiosis. Anat Rec. 1933; 57:339–343.
18. Liu K, et al. Origin of dendritic cells in peripheral lymphoid organs of mice. Nat Immunol. 2007; 8:578–583. [PubMed: 17450143]
19. Zhu SN, Chen M, Jongstra-Bilen J, Cybulsky MI. GM-CSF regulates intimal cell proliferation in nascent atherosclerotic lesions. J Exp Med. 2009; 206:2141–2149. [PubMed: 19752185]
20. Rosenfeld ME, Ross R. Macrophage and smooth muscle cell proliferation in atherosclerotic lesions of WHHL and comparably hypercholesterolemic fat-fed rabbits. Arteriosclerosis. 1990; 10:680–687. [PubMed: 2403295]
21. Gordon D, Reidy MA, Benditt EP, Schwartz SM. Cell proliferation in human coronary arteries. Proc Natl Acad Sci U S A. 1990; 87:4600–4604. [PubMed: 1972277]
22. Rekhter MD, Gordon D. Active proliferation of different cell types, including lymphocytes, in human atherosclerotic plaques. Am J Pathol. 1995; 147:668–677. [PubMed: 7677178]
23. Katsuda S, Coltrera MD, Ross R, Gown AM. Human atherosclerosis. IV. Immunocytochemical analysis of cell activation and proliferation in lesions of young adults. Am J Pathol. 1993; 142:1787–1793. [PubMed: 8099470]
24. Lutgens E, et al. Atherosclerosis in APOE*3-Leiden transgenic mice: from proliferative to atheromatous stage. Circulation. 1999; 99:276–283. [PubMed: 9892595]

25. Lutgens E, et al. Biphasic pattern of cell turnover characterizes the progression from fatty streaks to ruptured human atherosclerotic plaques. Cardiovasc Res. 1999; 41:473–479. [PubMed: 10341847]
26. Aikawa M, et al. An HMG-CoA reductase inhibitor, cerivastatin, suppresses growth of macrophages expressing matrix metalloproteinases and tissue factor in vivo and in vitro. Circulation. 2001; 103:276–283. [PubMed: 11208689]
27. Butcher MJ, Herre M, Ley K, Galkina E. Flow cytometry analysis of immune cells within murine aortas. J Vis Exp. 2011
28. Gough PJ, et al. Analysis of macrophage scavenger receptor (SR-A) expression in human aortic atherosclerotic lesions. Arterioscler Thromb Vasc Biol. 1999; 19:461–471. [PubMed: 10073945]
29. Teupser D, et al. Scavenger receptor activity is increased in macrophages from rabbits with low atherosclerotic response: studies in normocholesterolemic high and low atherosclerotic response rabbits. Arterioscler Thromb Vasc Biol. 1999; 19:1299–1305. [PubMed: 10323783]
30. Hazen SL. Oxidized phospholipids as endogenous pattern recognition ligands in innate immunity. J Biol Chem. 2008; 283:15527–15531. [PubMed: 18285328]
31. Sakai M, et al. The scavenger receptor serves as a route for internalization of lysophosphatidylcholine in oxidized low density lipoprotein-induced macrophage proliferation. J Biol Chem. 1996; 271:27346–27352. [PubMed: 8910311]
32. Seimon TA, Obstfeld A, Moore KJ, Golenbock DT, Tabas I. Combinatorial pattern recognition receptor signaling alters the balance of life and death in macrophages. Proc Natl Acad Sci U S A. 2006; 103:19794–19799. [PubMed: 17167049]
33. Heil M, et al. Blood monocyte concentration is critical for enhancement of collateral artery growth. Am J Physiol Heart Circ Physiol. 2002; 283:H2411–9. [PubMed: 12388258]
34. Boesten LS, et al. Macrophage retinoblastoma deficiency leads to enhanced atherosclerosis development in ApoE-deficient mice. FASEB J. 2006; 20:953–955. [PubMed: 16585057]
35. Diez-Juan A, et al. Selective inactivation of p27(Kip1) in hematopoietic progenitor cells increases neointimal macrophage proliferation and accelerates atherosclerosis. Blood. 2004; 103:158–161. [PubMed: 14504088]
36. Murphy AJ, et al. ApoE regulates hematopoietic stem cell proliferation, monocytosis, and monocyte accumulation in atherosclerotic lesions in mice. J Clin Invest. 2011; 121:4138–4149. [PubMed: 21968112]
37. Dutta P, et al. Myocardial infarction accelerates atherosclerosis. Nature. 2012; 487:325–329. [PubMed: 22763456]
38. Van Rooijen N, Sanders A. Liposome mediated depletion of macrophages: mechanism of action, preparation of liposomes and applications. J Immunol Methods. 1994; 174:83–93. [PubMed: 8083541]
39. Swirski FK, et al. Identification of splenic reservoir monocytes and their deployment to inflammatory sites. Science. 2009; 325:612–616. [PubMed: 19644120]
40. Galkina E, et al. Lymphocyte recruitment into the aortic wall before and during development of atherosclerosis is partially L-selectin dependent. J Exp Med. 2006; 203:1273–1282. [PubMed: 16682495]

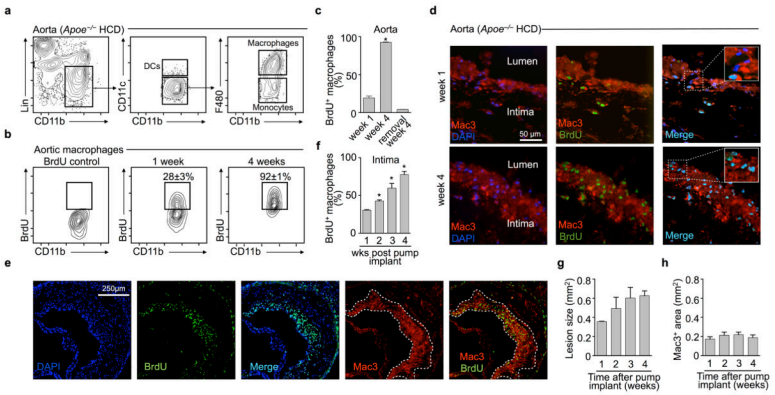

Figure 1. Macrophages turn over rapidly in lesions

(**a**) Identification of aortic macrophages in established atherosclerosis. Contour plots demonstrate gating scheme for aortic macrophages in *Apoe*$^{-/-}$ mice consuming HCD for 8 weeks. (**b**) BrdU-containing osmotic pumps were implanted in *Apoe*$^{-/-}$ mice consuming HCD for 8 weeks. Data depict BrdU incorporation in aortic macrophages 1 and 4 weeks following implantation of osmotic pumps. (**c**) Percentage of aortic macrophages that incorporate BrdU. Shown is quantification of data in b as well as BrdU^{+} macrophages in mice where pumps were removed for 4 weeks (mean ± SEM, n = 8 (week 1), n = 3 (week 4), n = 2 (week 4 removal)). (**d**) Immunofluorescence (IF) shows BrdU^{+} Mac3^{+} macrophages in aortic root lesions. (**e**) IF showing co-localization of BrdU and DAPI in intimal and adventitial macrophages of aortic root sections following 4 weeks of BrdU administration; 10x magnification. (**f**) Enumeration of BrdU^{+} Mac3^{+} macrophages by IF in aortic root sections (mean ± SEM, n = 2–3). * $P < 0.05$. (**g**) Lesion growth during BrdU labeling period. (**h**) Lesional macrophage content during BrdU labeling period. Data show area staining for Mac-3.

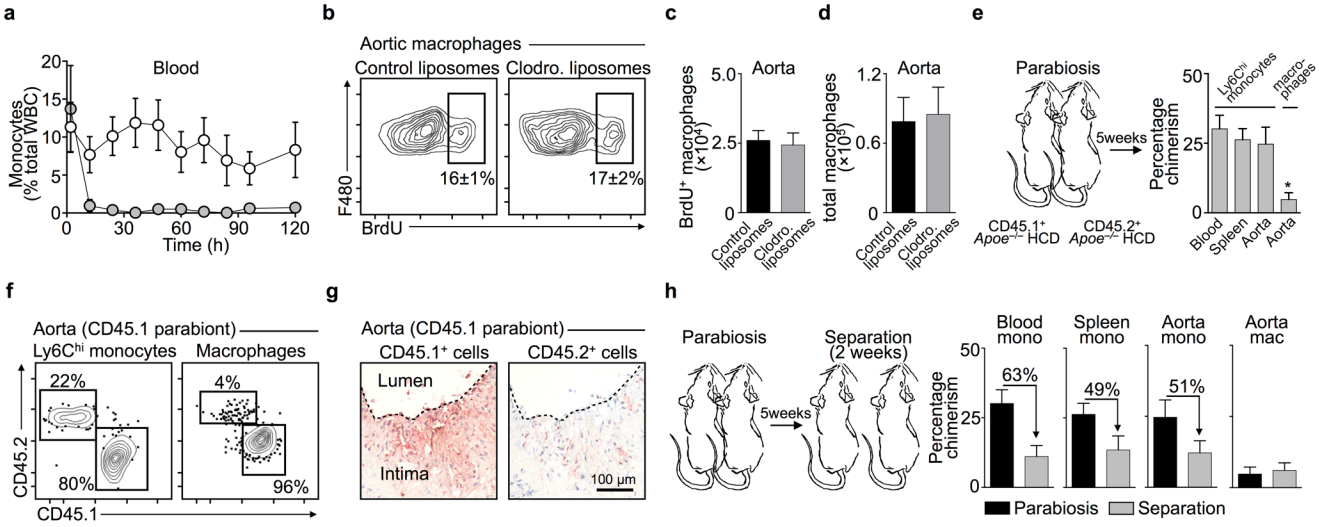

Figure 2. Lesional macrophage accumulation occurs largely independent of monocyte recruitment

(**a**) Effect of repeated clodronate liposome administration on peripheral blood monocytes (mean ± SEM, n = 4). (**b**) Effect of clodronate liposome treatment on BrdU incorporation by aortic macrophages. Data show percentage of $BrdU^+$ macrophages in aortic tissue following 5 d clodronate administration (mean ± SEM, n = 6–9). (**c**) Data show number of $BrdU^+$ macrophages in aortic tissue following 5 d clodronate treatment (mean ± SEM, n = 6–9). (**d**) Data show total number of macrophages in aortic tissue following 5 d clodronate treatment (mean ± SEM, n = 6–9). (**e**) $CD45.1^+$ and $CD45.2^+$ $Apoe^{-/-}$ HCD mice were joined in parabiosis for 5 weeks. Data show Ly-$6C^{high}$ monocyte chimerism in the blood, spleen, and aorta and macrophage chimerism in the aortic tissue (mean ± SEM; n = 6–8). (**f**) Representative contour plots demonstrate monocyte and macrophage chimerism in aortic tissue. (**g**) Immunohistochemistry (IHC) of aortic root sections showing CD45.1 and CD45.2 staining in $CD45.1^+$ parabionts. (**h**) $CD45.1^+$ and $CD45.2^+$ $Apoe^{-/-}$ HCD mice were joined in parabiosis for 5 weeks, separated and assessed for chimerism 2 weeks later. Shown is chimerism for monocytes in the blood, spleen, and aorta as well as macrophages in the aorta (mean ± SEM; n = 4–8).* $P < 0.05$.

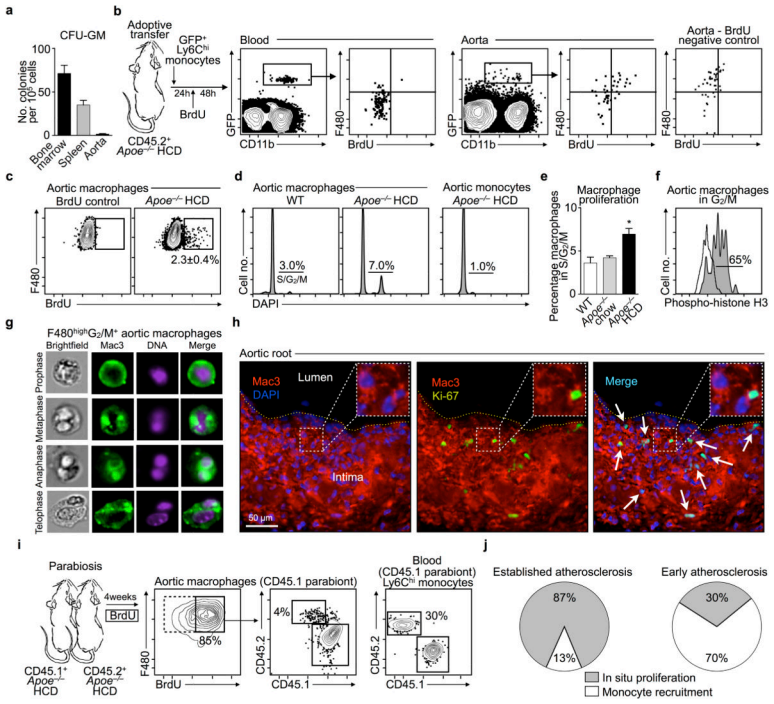

Figure 3. In situ proliferation dominates macrophage accumulation in atherosclerosis

(**a**) Data show colony-forming units–granulocytes and macrophages (CFU-GM) in spleen, bone marrow and aortic tissue of *Apoe*$^{-/-}$ HCD mice (mean ± SEM, n = 3). * $P < 0.05$. (**b**) BrdU incorporation following adoptive transfer of GFP^{+} Ly6C^{high} monocytes. One representative experiment is shown. (**c**) BrdU pulse labeling of aortic macrophages (mean ± SEM, n = 7). (**d**) Cell cycle analysis of aortic tissue macrophages. Histograms depict DAPI staining (mean ± SEM, n = 7). * $P < 0.05$. (**e**) Percentage of aortic tissue macrophages in S and G2/M phases of the cell cycle. (mean ± SEM, n = 3–7). * $P < 0.05$. (**f**) Phospho-histone H3 staining of aortic macrophages in G2/M phases of the cell cycle. (**g**) Analysis of aortic macrophages by ImageStreamX^{TM} imaging flow cytometry platform. Data depict actively dividing macrophages. (**h**) IF of aortic root sections demonstrating Ki-67 staining of Mac3^{+} intimal macrophages. (**i**) CD45.1^{+} and CD45.2^{+} *Apoe*$^{-/-}$ HCD mice were joined in parabiosis and then implanted with BrdU containing osmotic pumps. Data show chimerism in newly made (BrdU^{+}) aortic tissue macrophages. One representative experiment of two is shown. Monocyte chimerism in peripheral blood is also shown. (**j**) Relative contribution of in situ proliferation and monocyte recruitment to macrophage accumulation in early (2–3 month old) and established (4–5 months old) atherosclerosis.

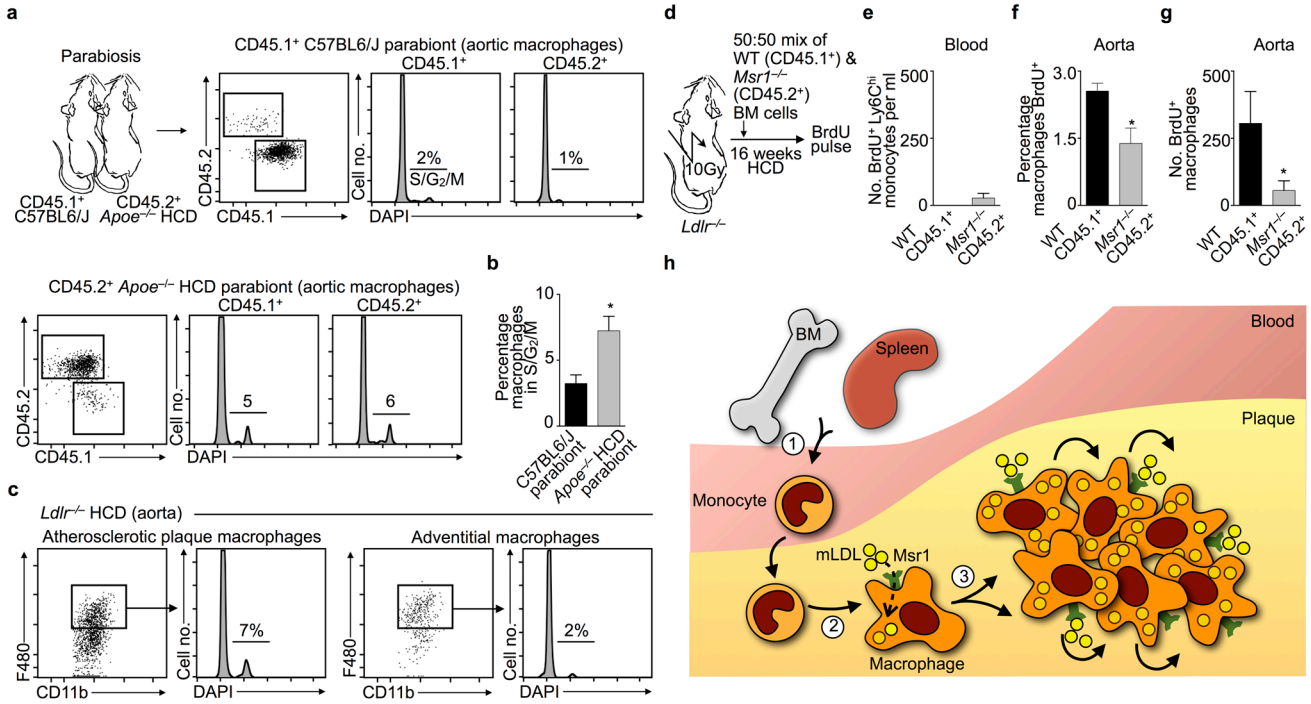

Figure 4. Lesion microenvironment dictates macrophage proliferation

(**a**) WT (CD45.1$^+$ C57BL6/J) and CD45.2$^+$ *Apoe*$^{-/-}$ HCD mice were joined in parabiosis for 5 weeks. Data show DAPI staining in CD45.1$^+$ and CD45.2$^+$ aortic tissue macrophages in each parabiont. One representative experiment of 3 is shown. (**b**) Enumeration of data in a. (mean ± SEM, n = 8–9). * P < 0.05. (**c**) Cell cycle analysis of intimal versus adventitial aortic macrophages. (**d**) WT/*Msr1*$^{-/-}$mixed chimeras were generated by reconstituting lethally irradiated *Ldlr*$^{-/-}$ mice with CD45.1$^+$ wild type (*Msr1*$^{+/+}$) and CD45.2$^+$ *Msr1*–deficient (*Msr1*$^{-/-}$) bone marrow cells. (**e**) Data show number of BrdU$^+$ *Msr1*$^{+/+}$ (WT) and BrdU$^+$ *Msr1*$^{-/-}$Ly6C^{high} monocytes in blood 2 h following BrdU pulse labeling. (mean ± SEM, n = 5). (**f**) Percentage of WT and *Msr1*$^{-/-}$ aortic macrophages that are BrdU$^+$. (mean ± SEM, n = 5).* P < 0.05. (**g**) Number of BrdU$^+$ *Msr1*$^{+/+}$and BrdU$^+$ *Msr1*$^{-/-}$ macrophages in aortic tissue of WT/*Msr1*$^{-/-}$ mixed chimeras. (mean ± SEM, n = 5).* *P* <0.05. (**h**) Cartoon depicting macrophage expansion in established atherosclerosis.